

NACA RM L52G23

NACA

TECH LIBRARY KAFB, NM  
0144359

# RESEARCH MEMORANDUM

EFFECTS OF WING ELASTICITY ON THE AERODYNAMIC  
CHARACTERISTICS OF A 45° SWEEPBACK-WING—  
FUSELAGE COMBINATION MEASURED IN THE  
LANGLEY 8-FOOT TRANSONIC TUNNEL

By Robert S. Osborne and John P. Mugler, Jr.

Langley Aeronautical Laboratory  
Langley Field, Va.

NATIONAL ADVISORY COMMITTEE  
FOR AERONAUTICS

WASHINGTON

September 17, 1952

319.98/13



## NATIONAL ADVISORY COMMITTEE FOR AERONAUTICS

## RESEARCH MEMORANDUM

EFFECTS OF WING ELASTICITY ON THE AERODYNAMIC  
CHARACTERISTICS OF A  $45^\circ$  SWEEPBACK-WING—  
FUSELAGE COMBINATION MEASURED IN THE  
LANGLEY 8-FOOT TRANSONIC TUNNEL

By Robert S. Osborne and John P. Mugler, Jr.

## SUMMARY

A wing-fuselage configuration employing a wing with  $45^\circ$  sweepback of the 0.25-chord line, aspect ratio of 4, taper ratio of 0.6, and NACA 65A006 airfoil sections has been tested with identical aluminum and steel wings at Mach numbers from 0.6 to 1.13 for angles of attack up to  $20^\circ$  to determine effects of wing elasticity. Dynamic pressures varied from 400 to 850 pounds per square foot.

The measured angles of wing-tip twist for the steel wing were approximately one-third those for the aluminum wing. This resulted in a maximum reduction in lift of 2 percent and a forward shift of the aerodynamic center of 3 percent of the mean aerodynamic chord for the aluminum wing-fuselage configuration as compared with the steel-wing-fuselage configuration. These effects were caused by twist due to wing bending rather than by twist due to aerodynamic torsional moments. Data for the wing-fuselage combination employing the steel wing were essentially free of aeroelastic effects for the conditions tested.

## INTRODUCTION

The bending of a sweptback wing due to positive lifting loads introduces effective twist which results in progressively decreased local angles of attack along the semispan from the root to the tip. This decrease would be expected to cause reductions in lift and drag and a forward inboard shift of the center of pressure. Some twist may also be produced by aerodynamic torsional moments. Its effects depend upon the location of the chordwise center of pressure relative to the flexural axis of the wing.

In reporting results of model tests of sweptback wings, these aeroelastic effects are usually estimated by some theoretical method in order that rigid-wing data may be presented. Relatively little information is available, however, on the actual measured effects of wing elasticity. Consequently, in the course of a relatively complete investigation of a wing-fuselage combination employing a wing with  $45^\circ$  sweepback of the 0.25-chord line, an aspect ratio of 4, a taper ratio of 0.6, and NACA 65A006 airfoil sections, which was conducted in the Langley 8-foot transonic tunnel, aluminum and steel models of the wing were tested in turn on the same body. Force and moment characteristics, base pressures, and angles of wing-tip twist were obtained.

The general aerodynamic characteristics of the fuselage alone and the configuration employing the steel wing are reported in reference 1. The aluminum-wing results are presented in this paper and are compared with the steel-wing data for angles of attack up to  $20^\circ$  at Mach numbers from 0.6 to 1.13.

#### SYMBOLS

$C_D$	drag coefficient
$C_L$	lift coefficient
$C_m$	pitching-moment coefficient about 0.25 $\bar{c}$
$\frac{\partial C_m}{\partial C_L}$	static longitudinal stability parameter
$C_N$	normal-force coefficient
$b$	wing span, in.
$c$	airfoil chord parallel to plane of symmetry, in.
$\bar{c}$	wing mean aerodynamic chord, in.
$c_{av}$	average wing chord, in.
$C_n$	wing-section normal-force coefficient
$M$	free-stream Mach number
$P_b$	base-pressure coefficient, $\frac{P_b - P_o}{q}$

$P_o$	free-stream static pressure, lb/sq ft
$P_b$	static pressure at model base, lb/sq ft
$q$	free-stream dynamic pressure, lb/sq ft
$R$	Reynolds number based on $\bar{c}$
$y$	lateral distance from model center line, in.
$\alpha$	angle of attack of fuselage center line, deg
$\delta$	wing deflection perpendicular to wing-chord plane, in.
$\theta$	angle of wing twist, deg (angle of attack of wing chord - $\alpha$ )
$\theta_t$	angle of wing-tip twist, deg (angle of attack of wing-tip chord - $\alpha$ )

## APPARATUS AND METHODS

### Tunnel

The investigation was conducted in the Langley 8-foot transonic tunnel, which is a dodecagonal slotted-throat, single-return wind tunnel operated at atmospheric stagnation pressures. The flow in the region of the test section occupied by the model was satisfactorily uniform at all Mach numbers (ref. 2).

### Model

Each of the two wings tested had  $45^\circ$  sweepback of the 0.25-chord line, an aspect ratio of 4, a taper ratio of 0.6, and NACA 65A006 airfoil sections parallel to the model plane of symmetry. One wing was constructed of solid 14ST aluminum alloy which has a modulus of elasticity of  $10.3 \times 10^6$  pounds per square inch, and the other was solid 6150 steel with a modulus of elasticity of  $30 \times 10^6$  pounds per square inch. The fuselage was a body of revolution with a fineness ratio of 9.8. It was of hollow steel construction. Dimensions of the model are shown in figure 1; further details are available in reference 1.

The two wings were tested in turn mounted on the center line of the fuselage at an angle of incidence of  $0^\circ$ . They were rigidly attached at the wing-fuselage juncture (14-percent wing semispan station).

### Model Support System

The model was attached to an internal strain-gage balance at its forward end. At its downstream end the balance was attached to an axial support tube through couplings which were varied to keep the model close to the center line of the tunnel at all angles of attack. A typical support configuration is shown in figure 2.

### Measurements and Accuracy

The test Mach number was determined from a calibration with respect to the pressure in the chamber surrounding the slotted test section and was estimated to be accurate within  $\pm 0.003$ .

Lift, drag, and pitching-moment coefficients were measured by means of a strain-gage balance located inside the fuselage and were estimated to be accurate within  $\pm 0.02$ ,  $\pm 0.002$ , and  $\pm 0.004$ , respectively, through the Mach number range. The regularity of the data and the ability to repeat it on successive runs indicated that the above estimates were conservative. The base-pressure coefficients were determined to within  $\pm 0.003$  by means of a static orifice located on the side of the sting support in the plane of the model base.

The angle of attack of the model was measured by a cathetometer sighted on a reference line on the side of the fuselage. It was estimated to be accurate within  $\pm 0.2^\circ$ . The angles of wing-tip twist were determined from measurements of the angles of attack of the wing tip obtained by sighting the cathetometer on a reference line at the tip. Because of vibration of the tip and the relatively short reference line, the accuracy of the angles of wing-tip twist was probably limited to approximately  $\pm 0.3^\circ$ .

### Test Conditions

The tests were conducted through a continuous Mach number range from 0.6 to approximately 1.13. The dynamic pressure varied from 400 to 850 pounds per square foot (fig. 3(a)), and the Reynolds number based on the wing mean aerodynamic chord was of the order of  $2 \times 10^6$  (fig. 3(b)). The configuration with the aluminum wing was tested at angles of attack from  $-2^\circ$  to  $20^\circ$  at intervals of  $2^\circ$  up to  $12^\circ$  angle of attack and  $4^\circ$  at the higher angles. The steel wing was tested at intervals of  $4^\circ$  over the angle range.

## CORRECTIONS

## Boundary Interference

At subsonic speeds the slotted test section minimized boundary interference effects such as blockage and boundary-induced upwash. At Mach numbers from 1.04 to 1.10, boundary-reflected disturbances altered the drag and pitching-moment coefficients as much as 0.002 and 0.005, respectively, in some instances. However, the data plotted against Mach number have been faired to eliminate these errors, and it is believed that none of the general trends exhibited by the faired data or the conclusions drawn therefrom were affected by these boundary-reflected disturbances. The base pressures were probably influenced by boundary interference at Mach numbers from 1.06 to 1.10. No corrections have been applied, however. A more detailed discussion of boundary-interference effects on the present model is contained in reference 1.

## Tares

By comparison with a tare investigation made on a similar model, it was estimated that the presence of the sting reduced the drag coefficient approximately 0.004 and increased the base-pressure coefficient on the order of 0.1 (see ref. 1). No corrections have been applied, however, since they are approximate only and would have no effect on the comparisons presented herein.

## RESULTS AND DISCUSSION

## Relative Effects of Bending and Torsion

Since the twist of a sweptback wing may be due to a combination of wing bending and torsional moments, discussion of the results presented herein requires an estimation of the relative contribution of each factor.

Consideration of the aerodynamic torsional moments calculated from load distributions obtained on a wing-fuselage configuration with geometry identical to the present model and employing a wing with structural properties similar to those for the aluminum wing (ref. 3) indicated that the maximum twist due to torsion occurred at the highest test Mach numbers at medium angles of attack. By employing a method outlined in reference 4, the spanwise distribution of wing twist was calculated for the aluminum wing at angles of attack of  $8^\circ$  and  $20^\circ$  for a Mach number of 1.11. Location of the effective root was determined from static bending tests and

a shear modulus of elasticity of  $3.9 \times 10^6$  pounds per square inch was used. The results are shown in figure 4, which also includes the spanwise variation of the location of the chordwise center of pressure with respect to the flexural axis.

As would be expected from the closeness of the centers of pressure to the flexural axis, the twist due to torsion was very small. The value at the tip was only  $0.13^\circ$  at an angle of attack of  $8^\circ$  and  $0.07^\circ$  at an angle of attack of  $20^\circ$ . Since the twist for the steel wing would be only approximately 35 percent of that for the aluminum wing, it may be assumed that, for the present wings, twist due to aerodynamic torsional moments was negligible and the measured effects of elasticity were due to wing bending only.

#### Wing-Tip Twist

The measured angles of wing-tip twist for the aluminum and steel wings are presented at constant angle of attack in figure 5. The negative values indicated reductions in local angle of attack with respect to the wing root. Increases in the magnitude of the twist with increasing Mach number were associated with outboard shifts in span loading and increases in total wing lift. At constant Mach number the twist increased with increases in angle of attack up to  $12^\circ$ . At higher angles the changes in twist were small because of reductions in lift-curve slope and inboard shifts of spanwise loading resulting from the inward spread of the region of separated flow at the tip. The unexpectedly low values of tip twist at an angle of attack of  $20^\circ$  are believed to be due to the measurement inaccuracies previously discussed.

Comparison of the tip twist for the two wings indicated that the values for the steel wing averaged approximately 32 percent of those for the aluminum wing. The comparative rigidity of the steel wing was shown by the twist not exceeding approximately  $-1^\circ$  for lift coefficients as high as 1.1; values for the aluminum wing were as large as  $-2.5^\circ$ .

#### Aerodynamic Characteristics

Lift.— Lift coefficients at constant angle of attack and constant Mach number are compared for the wing-fuselage configurations with the steel and aluminum wings in figures 6(a) and 7(a), respectively. At Mach numbers below 0.9 the differences in bending between the two wings had no significant effect on lift up to the highest angle of attack tested. For Mach numbers above 0.9 the lift coefficients for the aluminum-wing configuration were approximately 2 percent lower than those for the steel-wing model at angles of attack above  $6^\circ$ . The apparent small increase in lift for the aluminum wing over the steel wing at an angle of attack of  $4^\circ$  (fig. 6(a)) was probably due to inadvertent differences in angle of attack.

The measured differences in lift between the two wings were smaller than those predicted for the linear portion of the lift curve by the theoretical method of reference 5. The latter method indicated reductions in lift coefficient between the steel and aluminum wing-fuselage combinations varying from 3 percent at a Mach number of 0.6 to 6 percent at a Mach number of 1.11. Another estimation of the reduction in lift was made by employing a calculated spanwise variation of wing twist and weighting the reduction in local angle of attack with the local chord. The change in effective model angle of attack was determined to be 49 percent of the tip twist. Differences in the measured angles of wing-tip twist for the two wings, considered over the linear portion of the lift curve, again predicted reductions in lift varying from 3 to 6 percent for the aluminum configuration as compared with the steel configuration. Although the differences between the measured and calculated reductions in lift were relatively large, they were small in absolute magnitude and are not considered to indicate a failure of these approximate theoretical methods.

Drag.- For angles of attack of  $8^{\circ}$  and above the drag coefficients for the configuration with the steel wing were from 0.005 to 0.015 higher than those for the aluminum wing (fig. 6(b)). This was due to the higher lift for the steel wing, since the drag polars (fig. 7(b)) indicated no significant differences between the two wings. The slightly lower drag coefficients for the aluminum-wing-fuselage configuration at low lift coefficients, for example, would result in an increase in maximum lift-drag ratio of only approximately 5 percent for the configuration in a support-free, power-off condition (drag corrected for sting interference).

Pitching moment.- At positive angles of attack the larger tip twist for the aluminum wing resulted in more positive pitching-moment coefficients for the aluminum-wing-fuselage configuration as compared with the configuration employing the steel wing (figs. 6(c) and 7(c)). This was due to an inboard, forward movement of the center of pressure associated with decreased local angles of attack near the tip.

The variations of the static-longitudinal-stability parameter with Mach number (fig. 8) indicated that the aerodynamic center for the aluminum-wing-fuselage configuration was approximately 3 percent of the mean aerodynamic chord ahead of that for the steel-wing-fuselage configuration for lift coefficients up to that at which the unstable break in pitching moment occurred. The comparatively large forward shift at Mach numbers up to 0.8 for lift coefficients from 0.3 to 0.6 may have been due to angle-of-attack effects on the separation vortex which extends along the leading-edge of the wing for these test conditions (see ref. 1). The theoretical method of reference 5 predicted over the linear portion of the lift curve a forward movement of the aerodynamic center for the aluminum wing with respect to the steel wing which

~~CONFIDENTIAL~~



varied from 0.7 percent of the mean aerodynamic chord at a Mach number of 0.6 to 1.6 percent at a Mach number of 1.11.

At Mach numbers from 0.6 to 0.97 increased wing flexibility had no effect on the pitch-up tendency (fig. 7(c)). At higher Mach numbers the lift coefficient at which the unstable break in pitching moment occurred was increased approximately 0.05 and some reduction in the abruptness of the pitch-up was indicated at Mach numbers from 0.99 to 1.06.

Base pressure.- Comparison of the base-pressure coefficients for the configurations with the aluminum and steel wings (fig. 9) indicated no significant differences through the angle-of-attack and Mach number ranges tested.

Significance of results.- By assuming that the aeroelastic effects were proportional to the angles of wing-tip twist, it was indicated that differences in the force and moment characteristics between configurations employing a completely rigid wing and the present aluminum wing would be 150 percent of those measured for the steel and aluminum models, whereas, differences between data for the completely rigid- and the steel-wing configurations would be 50 percent of those for the models tested. As compared with a wing-fuselage combination employing a rigid wing, then, wing elasticity reduced the lift for the aluminum model a maximum of 3 percent and shifted the aerodynamic center forward about 4.5 percent of the mean aerodynamic chord; whereas for the steel model the lift was reduced a maximum of 1 percent and the aerodynamic center was moved forward 1.5 percent of the mean aerodynamic chord.

Aeroelastic effects on the steel wing were apparently very small, and it may be concluded that essentially rigid-wing data are obtained from solid steel wings with comparable or more favorable geometry and mounting conditions when tested at stagnation pressures which are no greater than atmospheric.

The significance of these results with reference to full-scale aircraft is somewhat limited due to large differences in dynamic pressure and wing structure. However, it is indicated that wing elasticity would cause some loss in lift-curve slope and a forward shift of the aerodynamic center for a full-scale wing. The effects of elasticity in relieving the abruptness of the unstable break in pitching moment would be of little importance, at least for the present wing, since the relieving effect occurred only at Mach numbers higher than those at which the most severe pitch-up was encountered (see fig. 7(c)).

### Theoretical Considerations

Spanwise deflection and twist.- By assuming the only structural deformation was that due to wing bending and using span-load distributions from reference 3, the spanwise variations of deflection of the 0.45-chord line and the angle of wing twist were calculated for the aluminum and steel wings at a Mach number of 1.11 for angles of attack of  $8^\circ$  and  $20^\circ$  (fig. 10). Although the spanwise distribution used applied strictly only to the aluminum wing, it probably also approximated the loading over the steel wing more closely than any available theoretical method. The effective roots in bending and the moments of inertia of the appropriate airfoil sections were determined by static bending tests of the two wings.

Wing-tip twist.- The angles of wing-tip twist were calculated for the two wings through the Mach number range of the tests for angles of attack of  $8^\circ$  and  $20^\circ$  and are compared with the measured values in figure 11. The data were in qualitative agreement, the changes in twist with Mach number being generally predicted by the calculations. The largest discrepancy between the magnitude of the measured and calculated twist occurred for the steel wing at an angle of attack of  $20^\circ$ . A study of the accuracy of the measured values and a comparison of the data at angles of attack of  $16^\circ$  and  $24^\circ$  (ref. 1) with that at  $20^\circ$  indicated that the disagreement was probably due more to inaccurate measurements of the twist angles than to a failure of the theoretical method. It may be concluded, therefore, that, if the span-load distribution is known, the changes in angle of attack along the semispan due to wing bending may be calculated with a satisfactory degree of accuracy.

Effects of support location.- Moving the support location of a sweptback wing inboard increases the twist over the outboard portions of the wing and extends the spanwise extent of decreased local angle of attack inboard. The effects of bending on the present wings were estimated for a wing-alone testing condition by comparing the calculated spanwise variation of twist for the wings mounted at the 14-percent-semispan station (fig. 10) with calculated spanwise variations assuming the wings mounted at the root chord and not in the presence of the fuselage. The results indicated that moving the support location 14-percent semispan inboard increased the tip twist by 40 percent and the reduction in effective angle of attack along the entire span by 75 percent. The steel wing of the present tests, then, although being effectively rigid when mounted on the fuselage, would probably exhibit appreciable aero-elastic effects when supported at the plane of symmetry.

## CONCLUSIONS

The following conclusions may be drawn from a wind-tunnel investigation of wing-fuselage combinations employing 45° sweptback wings constructed of steel and aluminum at transonic speeds:

1. Aeroelastic effects were due to wing bending. Twist due to aerodynamic torsional moments was negligible.
2. Wing twist for the steel wing was approximately one-third that for the aluminum wing. The differences in twist resulted in a maximum reduction in lift of 2 percent and a forward shift of the aerodynamic center of 3 percent of the mean aerodynamic chord for the aluminum-wing-fuselage combination as compared with the steel-wing-fuselage combination.
3. Solid steel wings with geometry and mounting conditions comparable with or more favorable than those of the present wings are essentially free of aeroelastic effects when tested at stagnation pressures which are no greater than atmospheric.
4. For conditions similar to those of these tests, if the span-load distribution is known, the spanwise variation of wing twist can be adequately predicted.
5. Calculations indicated that small inboard shifts of the mounting location result in large increases in wing bending effects.

Langley Aeronautical Laboratory  
National Advisory Committee for Aeronautics  
Langley Field, Va.

## REFERENCES

1. Osborne, Robert S., and Mugler, John P., Jr.: Aerodynamic Characteristics of a  $45^{\circ}$  Sweptback Wing-Fuselage Combination and the Fuselage Alone Obtained in the Langley 8-Foot Transonic Tunnel. NACA RM L52E14, 1952.
2. Ritchie, Virgil S., and Pearson, Albin O.: Calibration of the Slotted Test Section of the Langley 8-Foot Transonic Tunnel and Preliminary Experimental Investigation of Boundary-Reflected Disturbances. NACA RM L51K14, 1952.
3. Loving, Donald L., and Williams, Claude V.: Aerodynamic Loading Characteristics of a Wing-Fuselage Combination Having a Wing of  $45^{\circ}$  Sweepback Measured in the Langley 8-Foot Transonic Tunnel. NACA RM L52B27, 1952.
4. Gray, W. H., and Allis, A. E.: The Torsional Deflections of Several Propellers Under Operating Conditions. NACA RM L51A19, 1951.
5. Diederich, Franklin W., and Foss, Kenneth A.: Charts and Approximate Formulas for the Estimation of Aeroelastic Effects on the Loading of Swept and Unswept Wings. NACA TN 2608, 1952.

## Wing Details

Airfoil section  
 (parallel to plane of symmetry) NACA 65A006  
 Area, sq ft 1  
 Aspect ratio 4  
 Taper ratio 0.6  
 Incidence, deg 0  
 Dihedral, deg 0

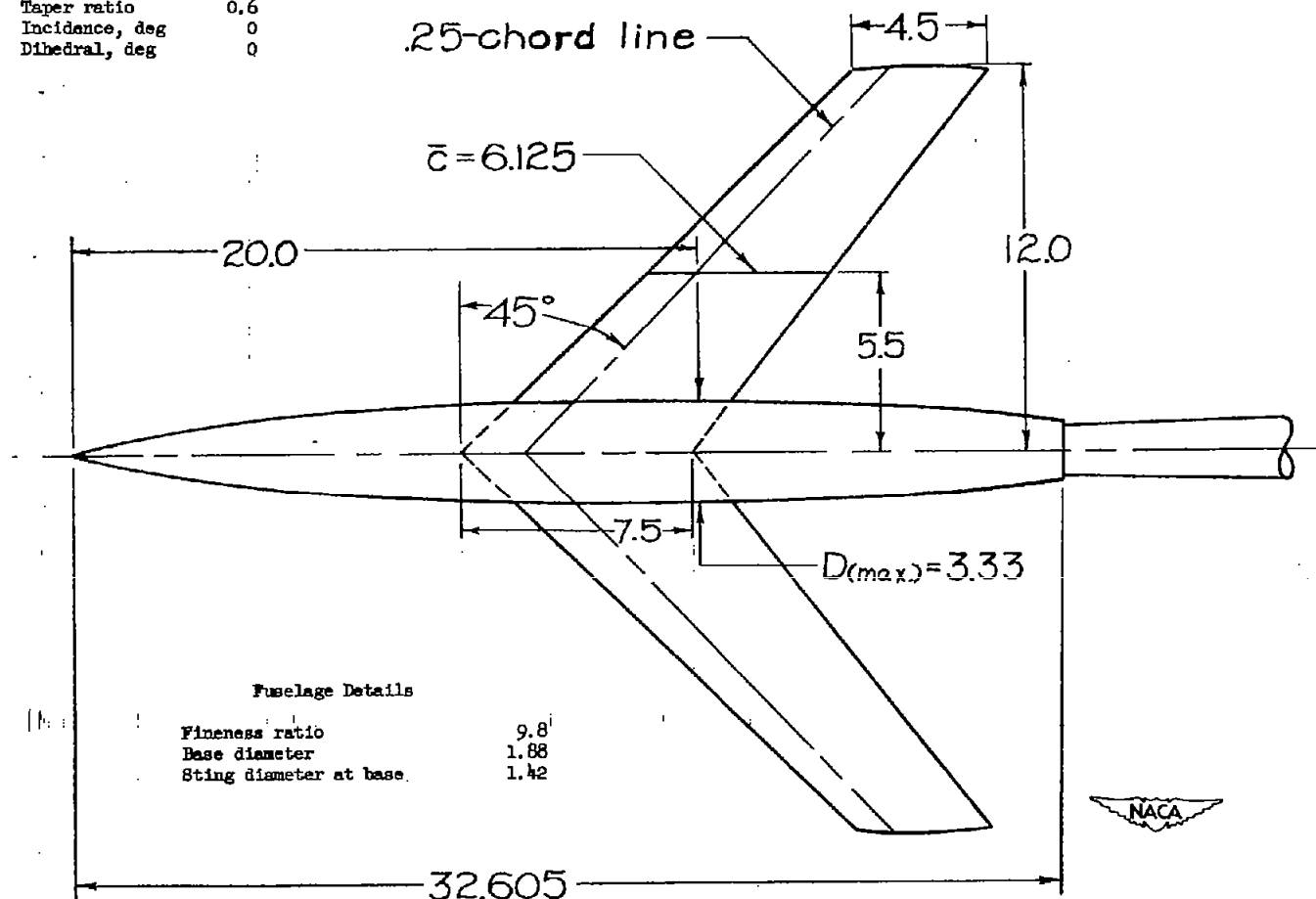


Figure 1.- Model details. All dimensions in inches.

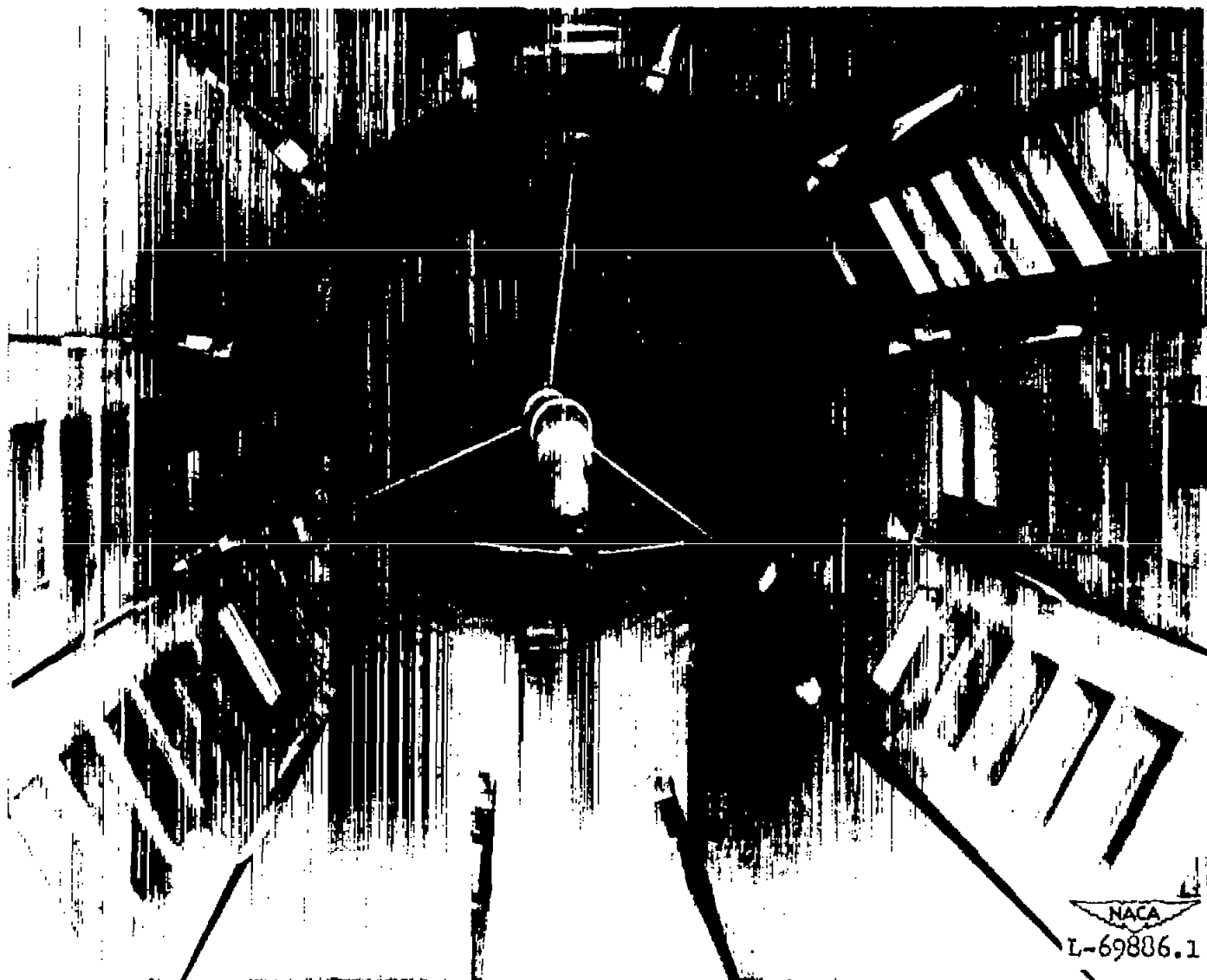


Figure 2.- Model and support system in the Langley 8-foot transonic tunnel.

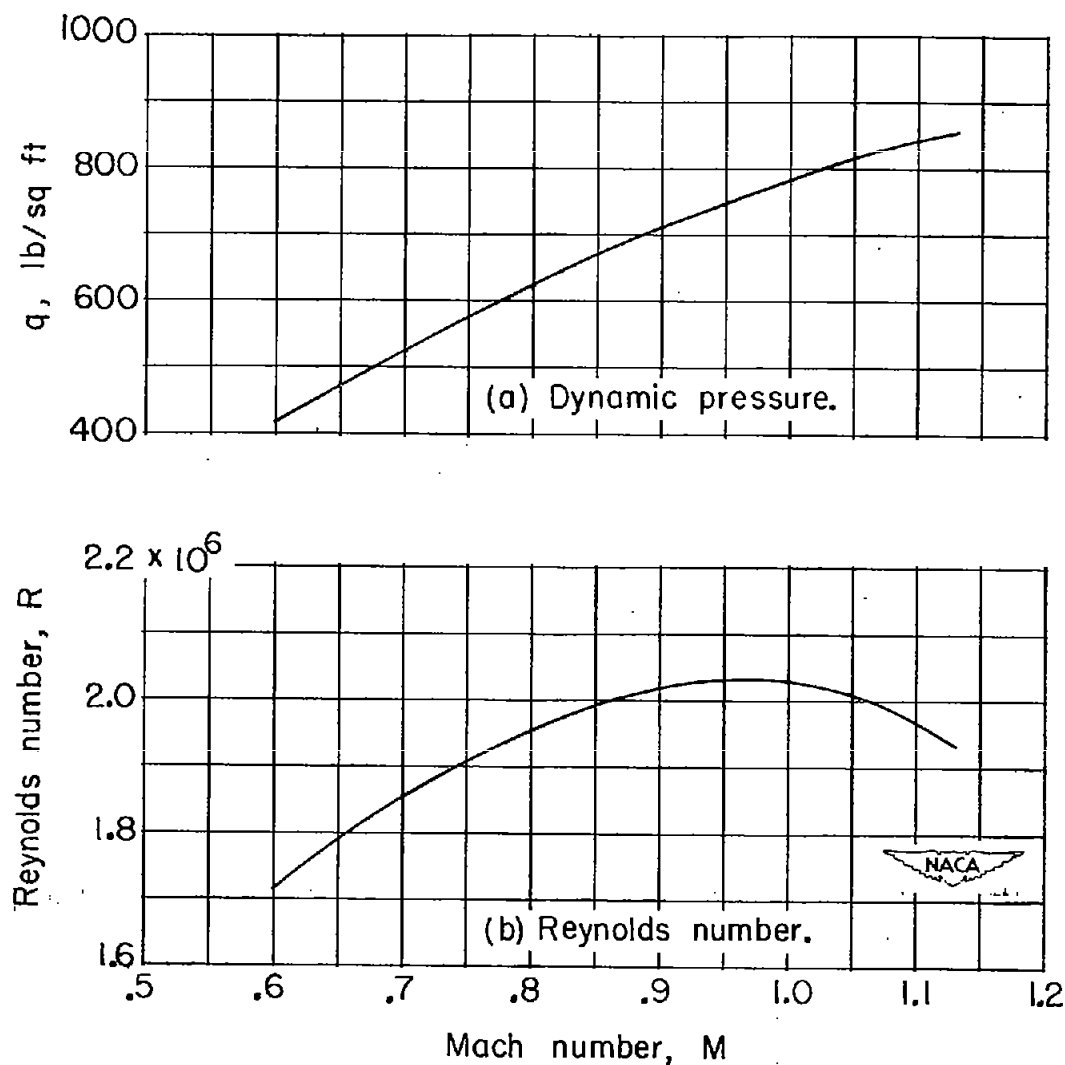


Figure 3.- Typical variation with Mach number of dynamic pressure and Reynolds number based on a wing mean aerodynamic chord of 6.125 inches.

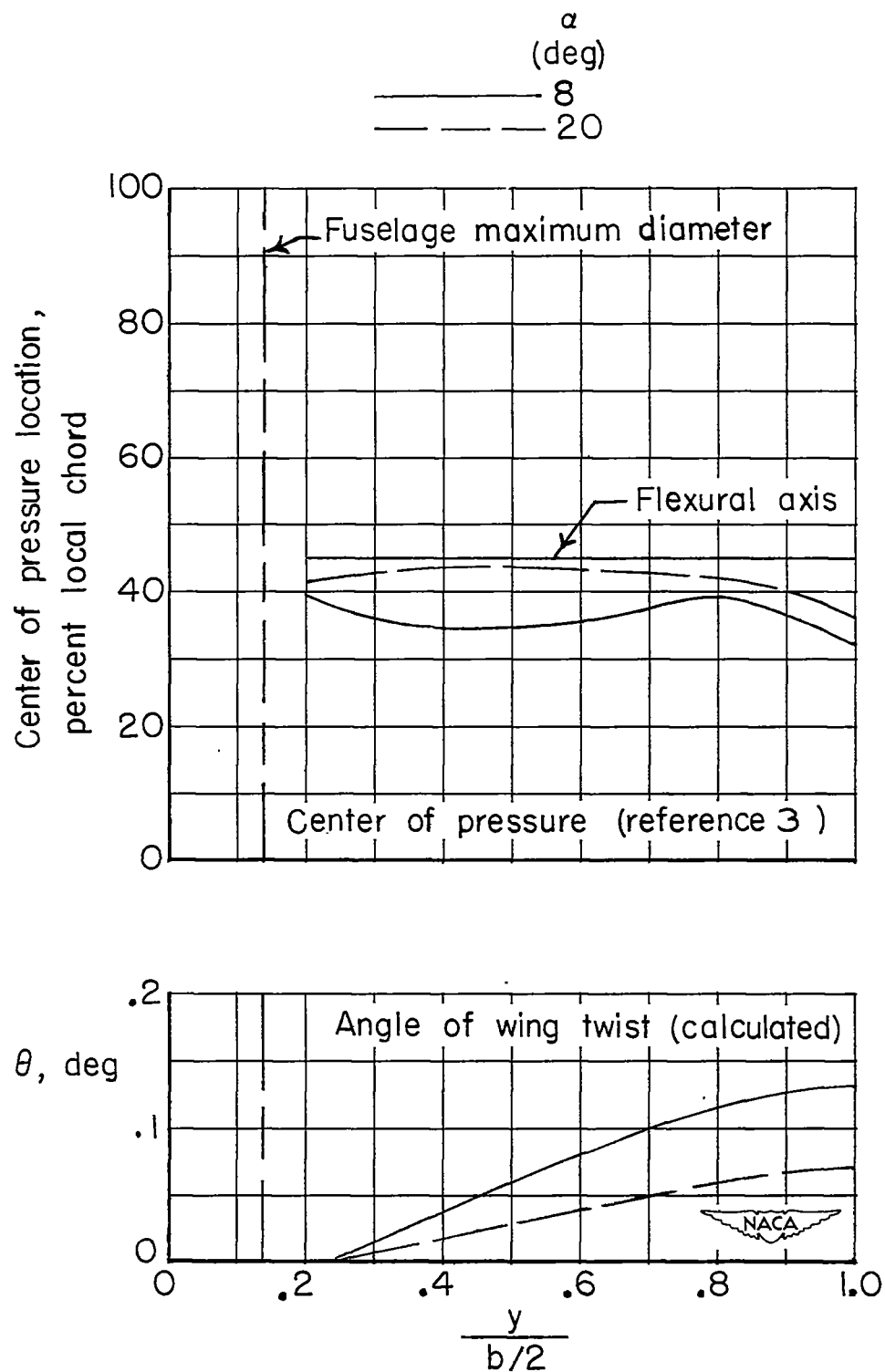


Figure 4.- Calculated angles of wing twist due to aerodynamic torsional moments for the aluminum wing at a Mach number of 1.11.



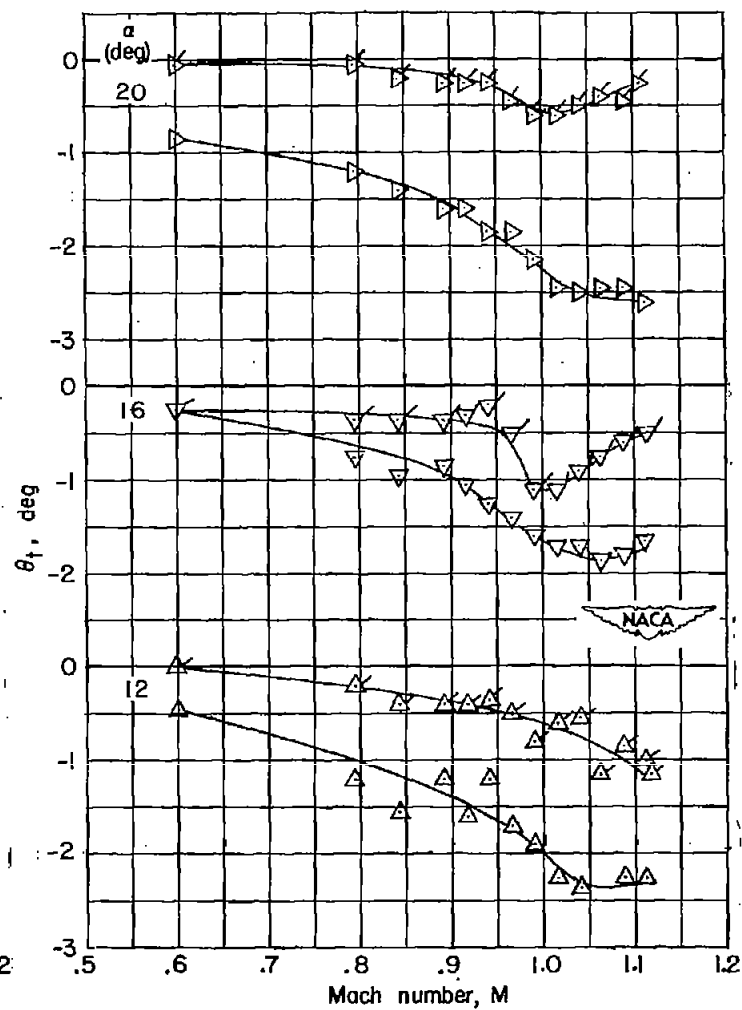
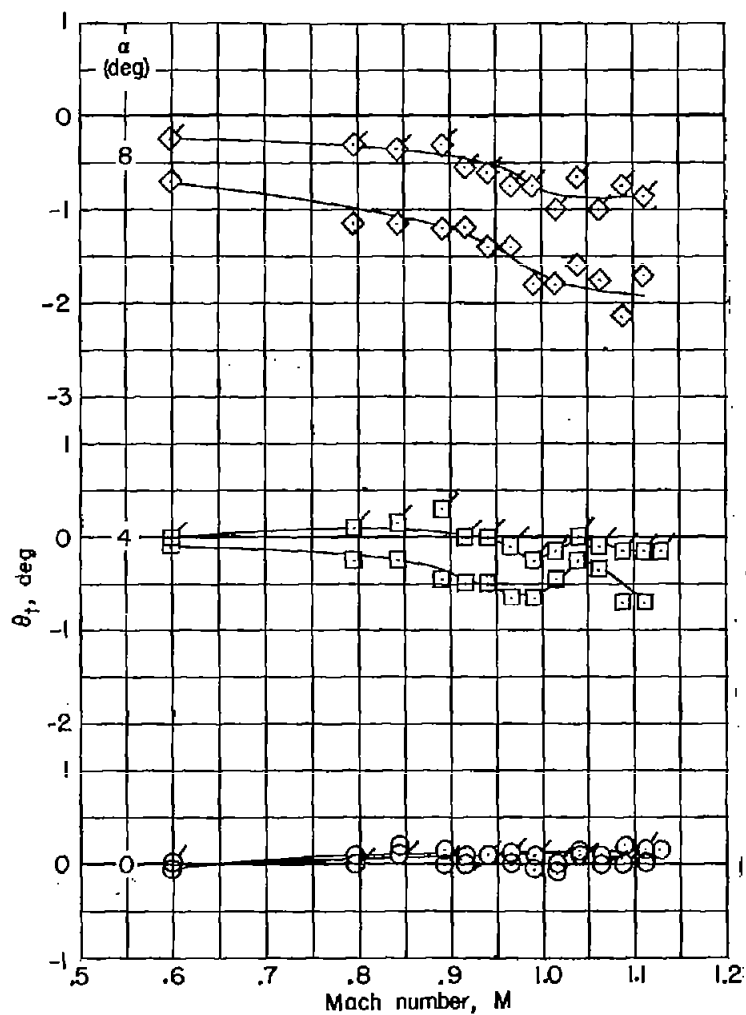
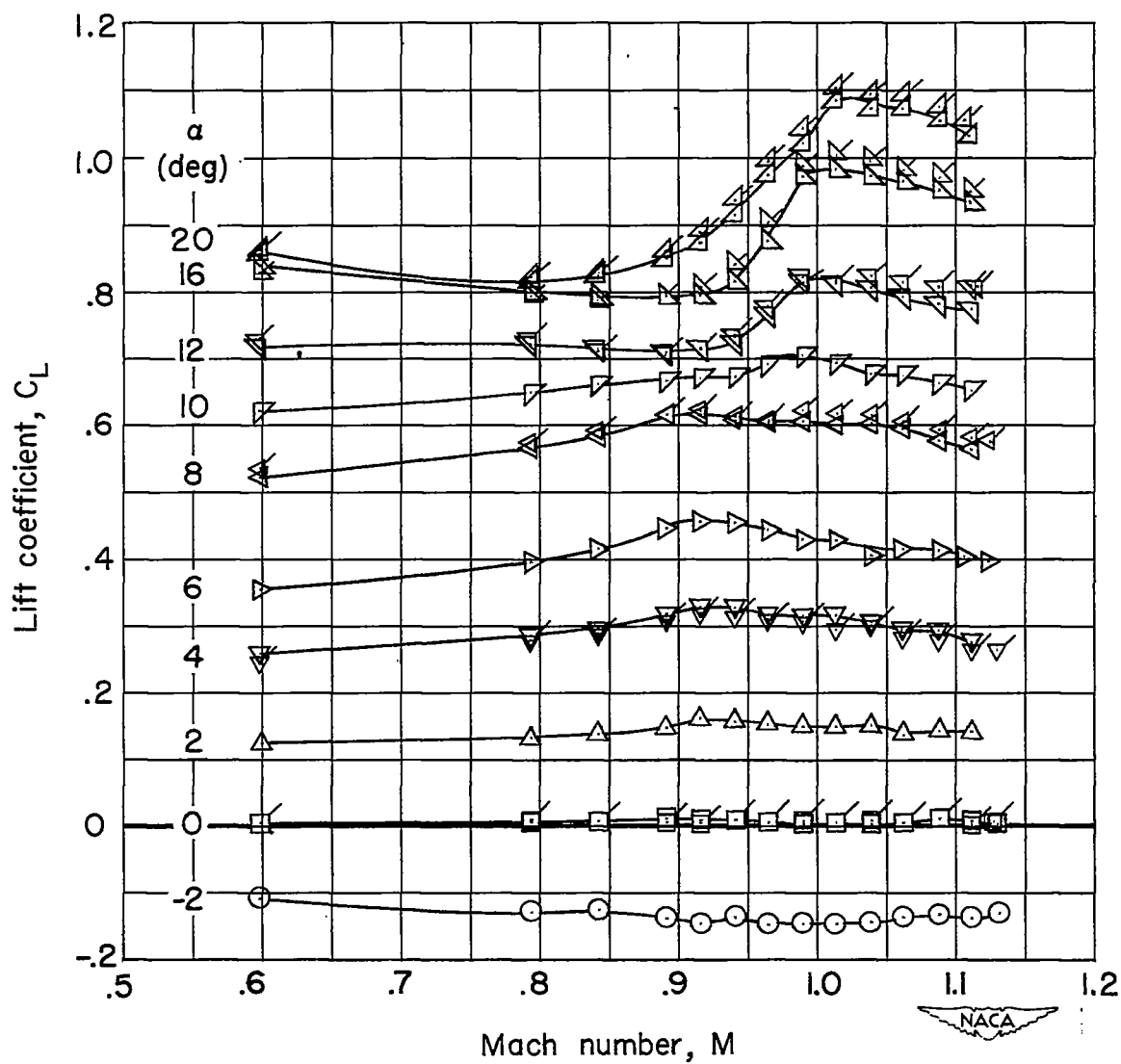
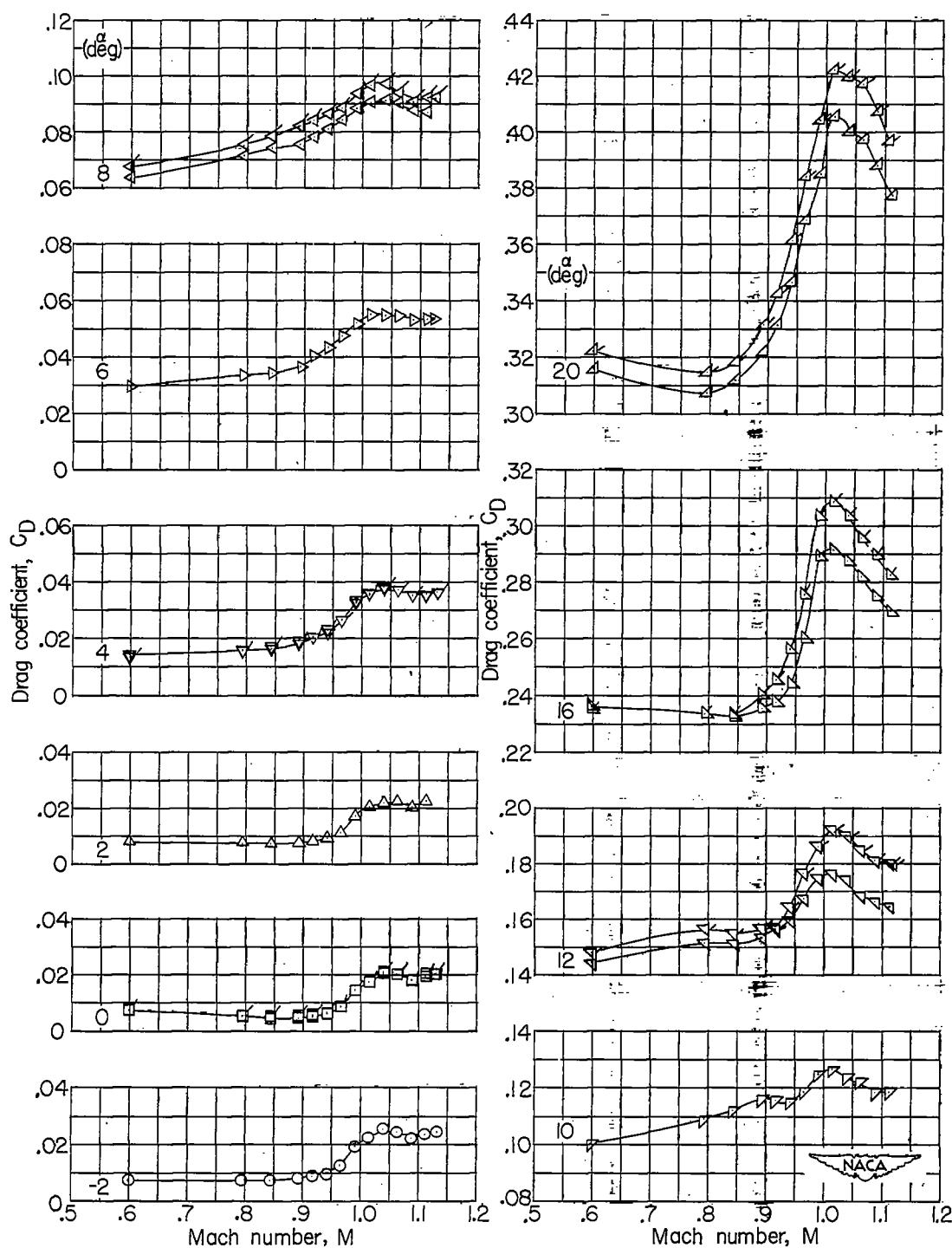


Figure 5.- Variation with Mach number of measured angles of wing-tip twist for the aluminum and steel wings. Flagged symbols indicate steel-wing data.



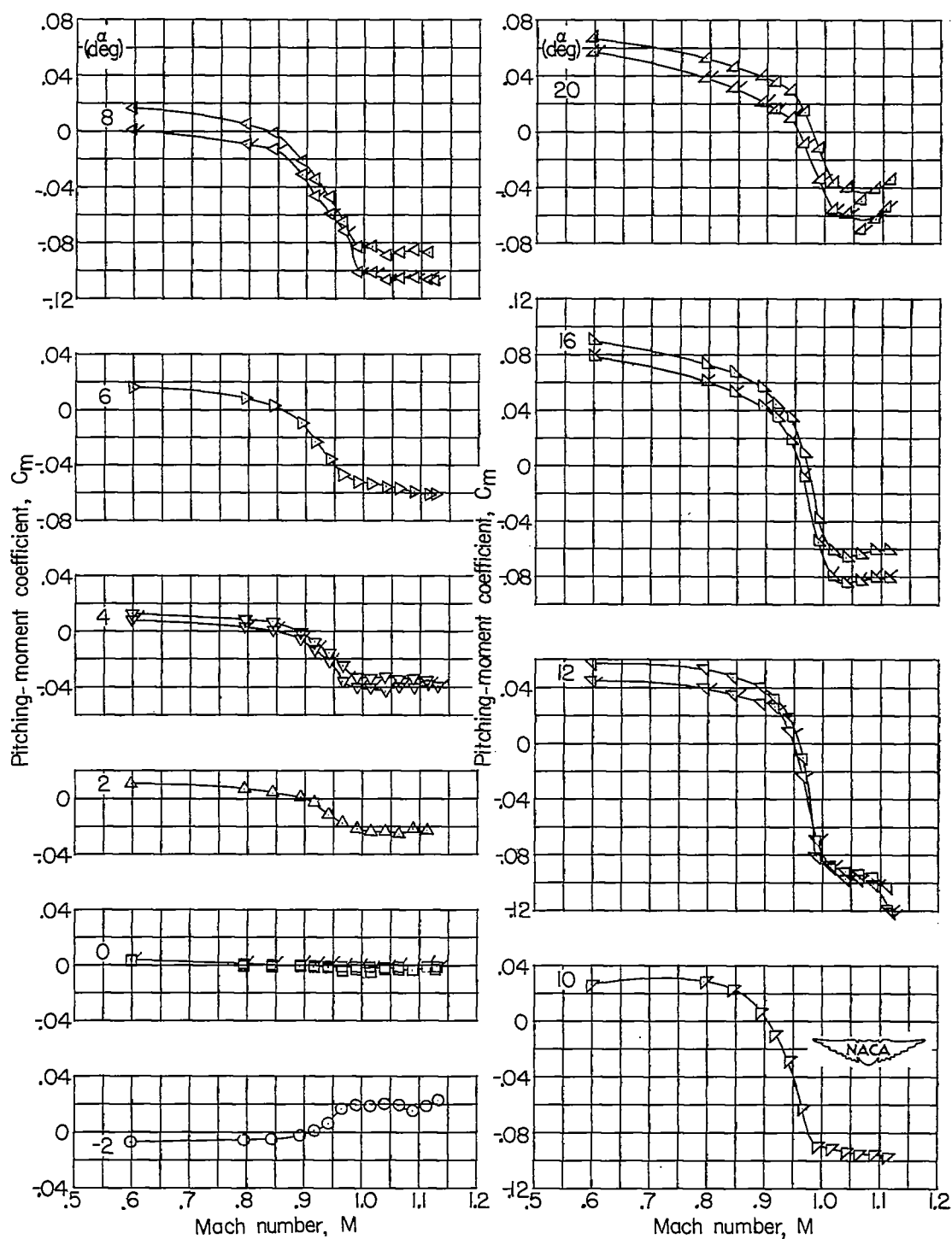
(a) Lift coefficient.

Figure 6.- Variation with Mach number of the force and moment characteristics for the aluminum- and steel-wing-fuselage configurations. Flagged symbols indicate steel-wing data.



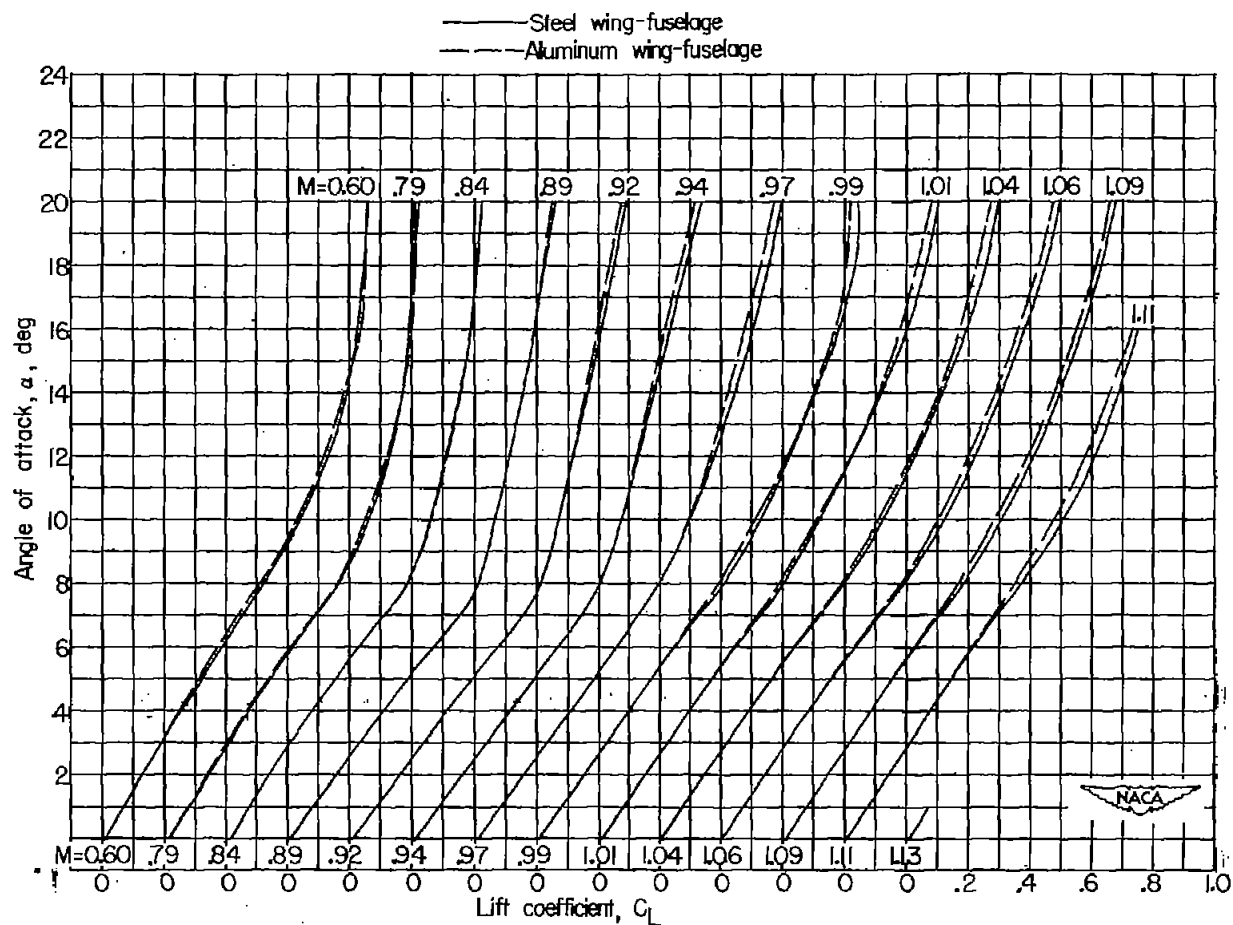
(b) Drag coefficient.

Figure 6.- Continued.



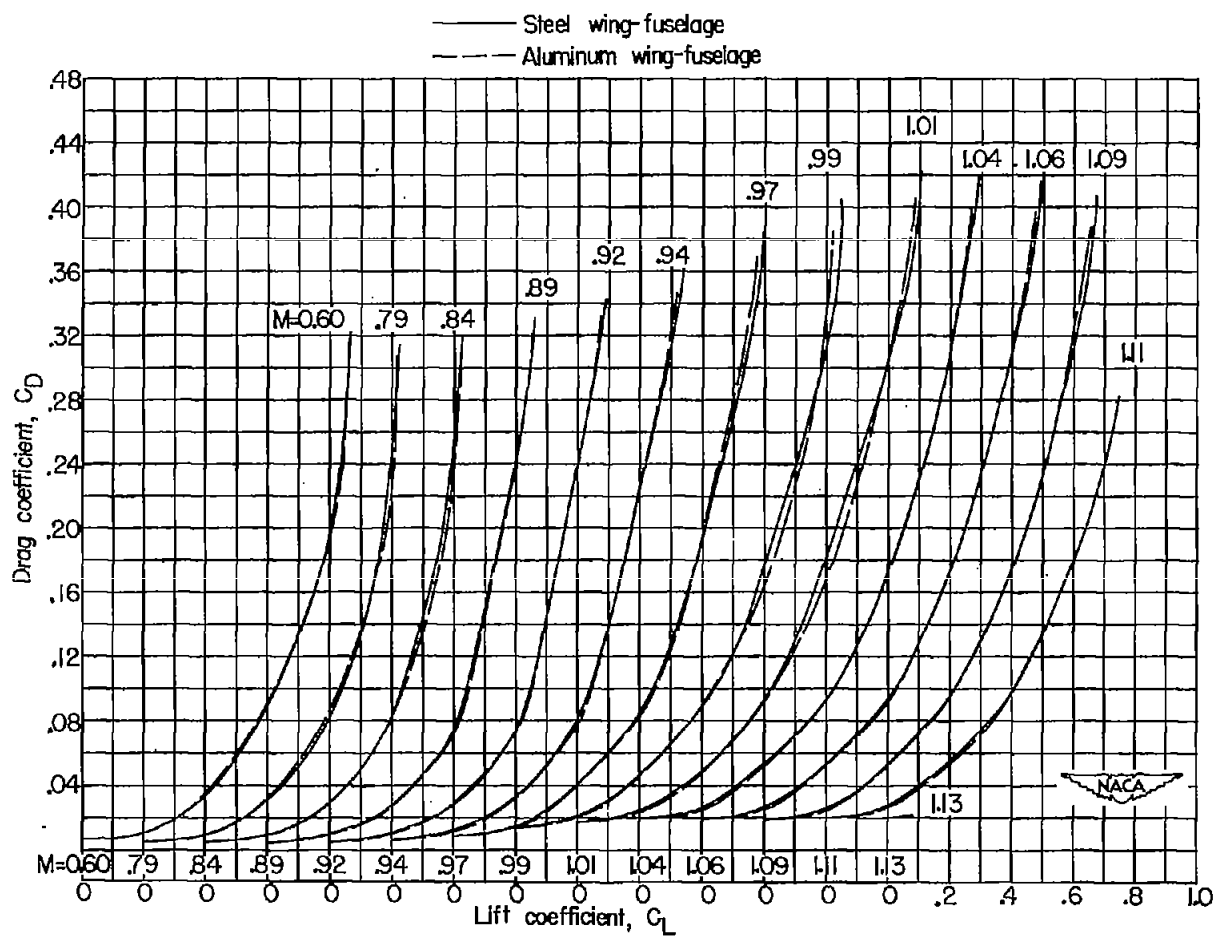
(c) Pitching-moment coefficient.

Figure 6.- Concluded.



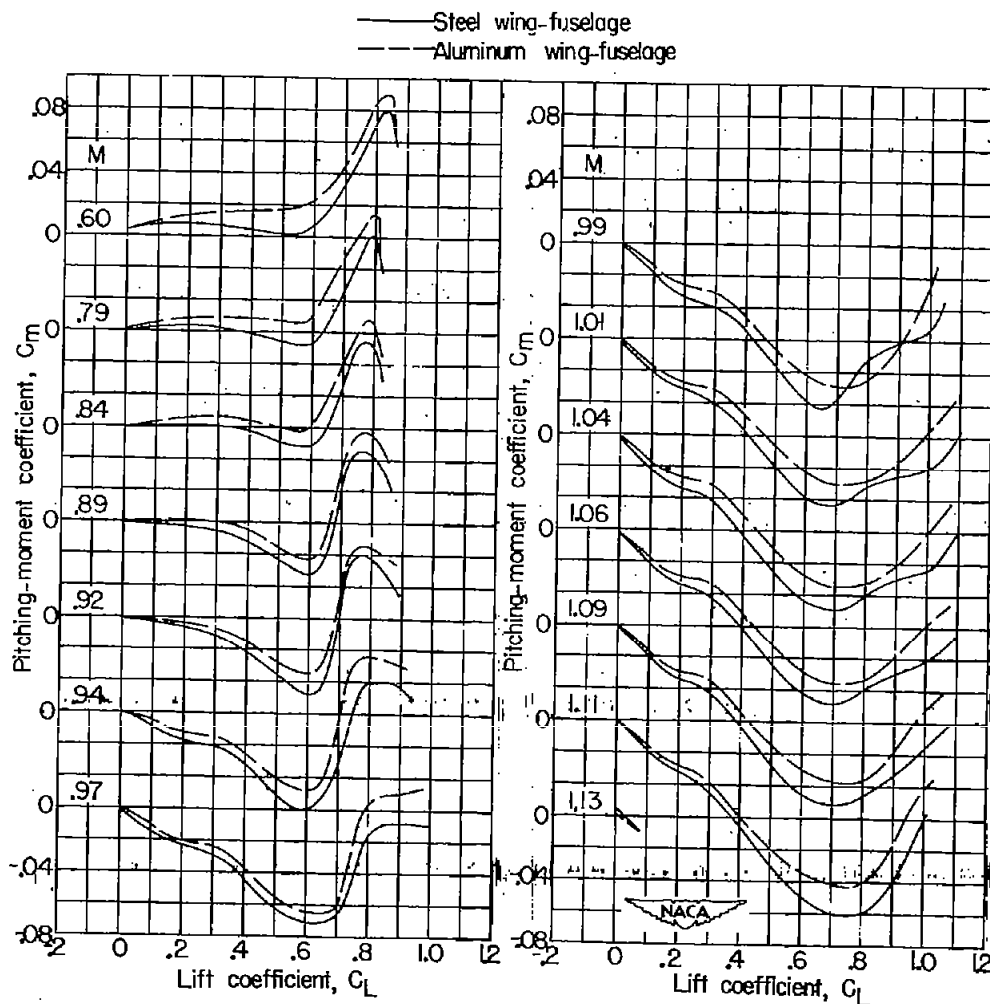
(a) Angle of attack.

Figure 7.- Variation with lift coefficient of the force and moment characteristics for the aluminum- and steel-wing-fuselage configurations.



(b) Drag coefficient.

Figure 7.- Continued.



(c) Pitching-moment coefficient.

Figure 7.- Concluded.

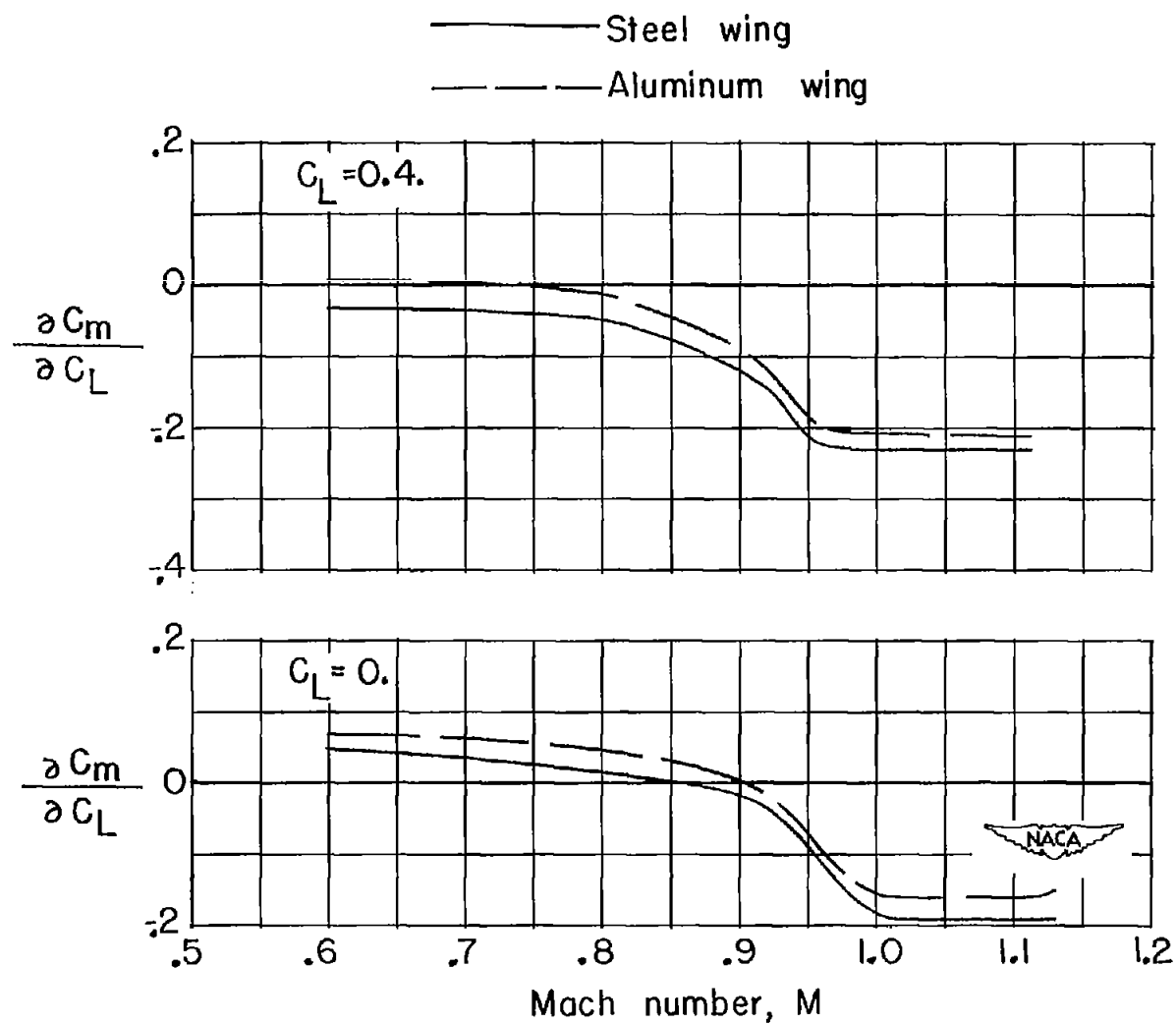


Figure 8.- Variation with Mach number of the longitudinal stability parameter for the aluminum- and steel-wing-fuselage configurations.



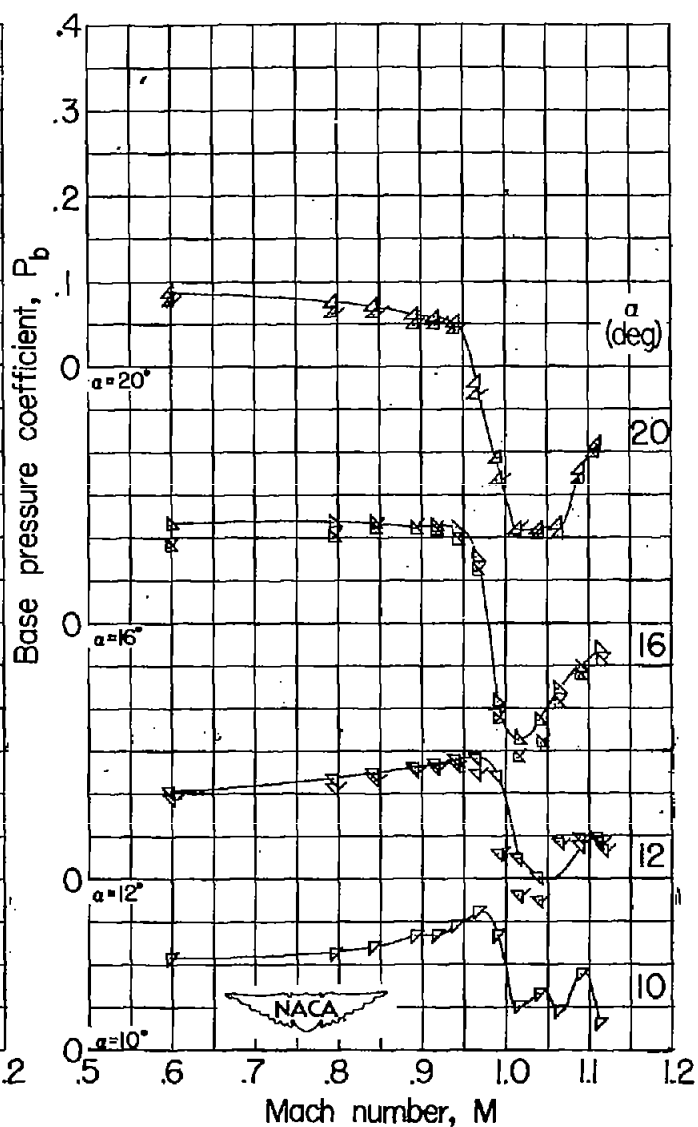
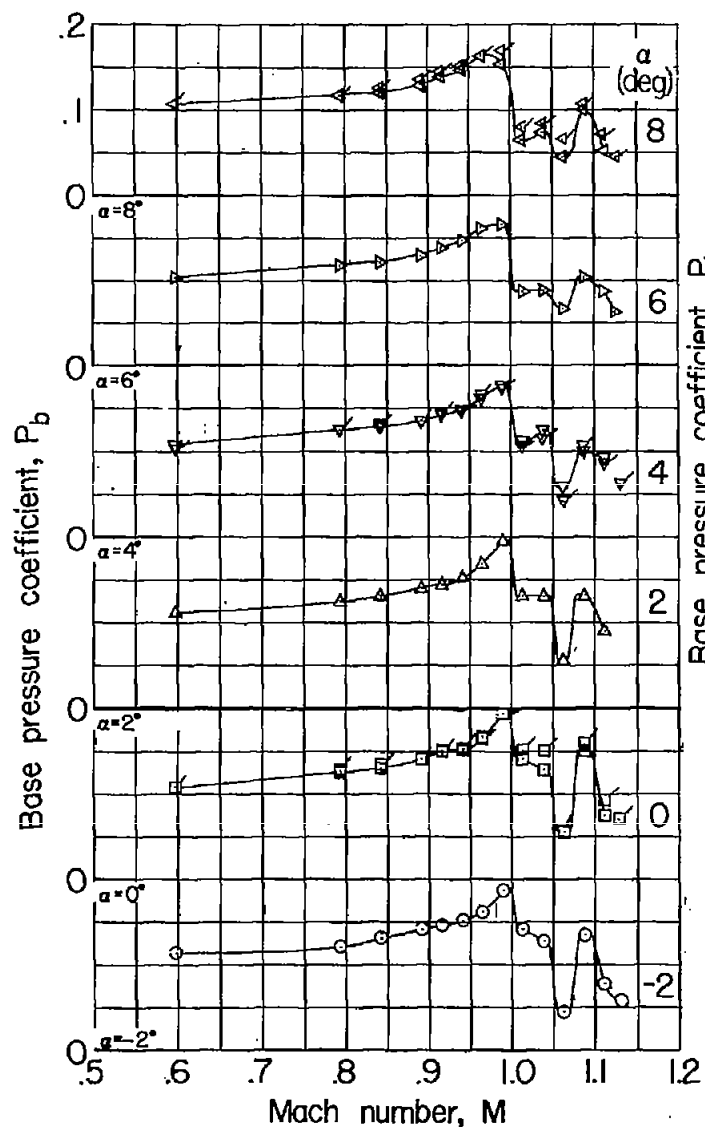


Figure 9.- Variation with Mach number of the base pressure coefficients for the aluminum- and steel-wing-fuselage configurations. Flagged symbols indicate steel-wing data.

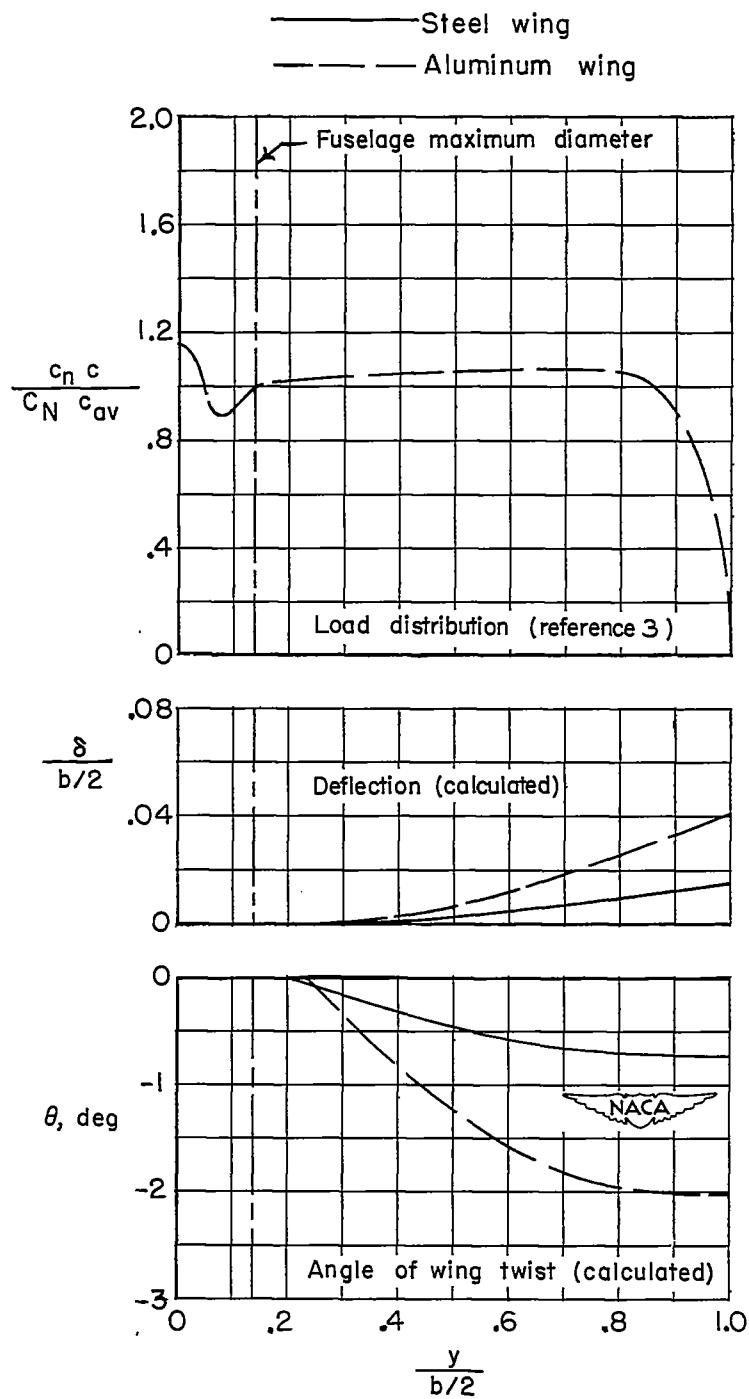
(a)  $\alpha = 8^\circ$ .

Figure 10.- Calculated deflections and angles of wing twist due to bending for the aluminum and steel wings at a Mach number of 1.11.

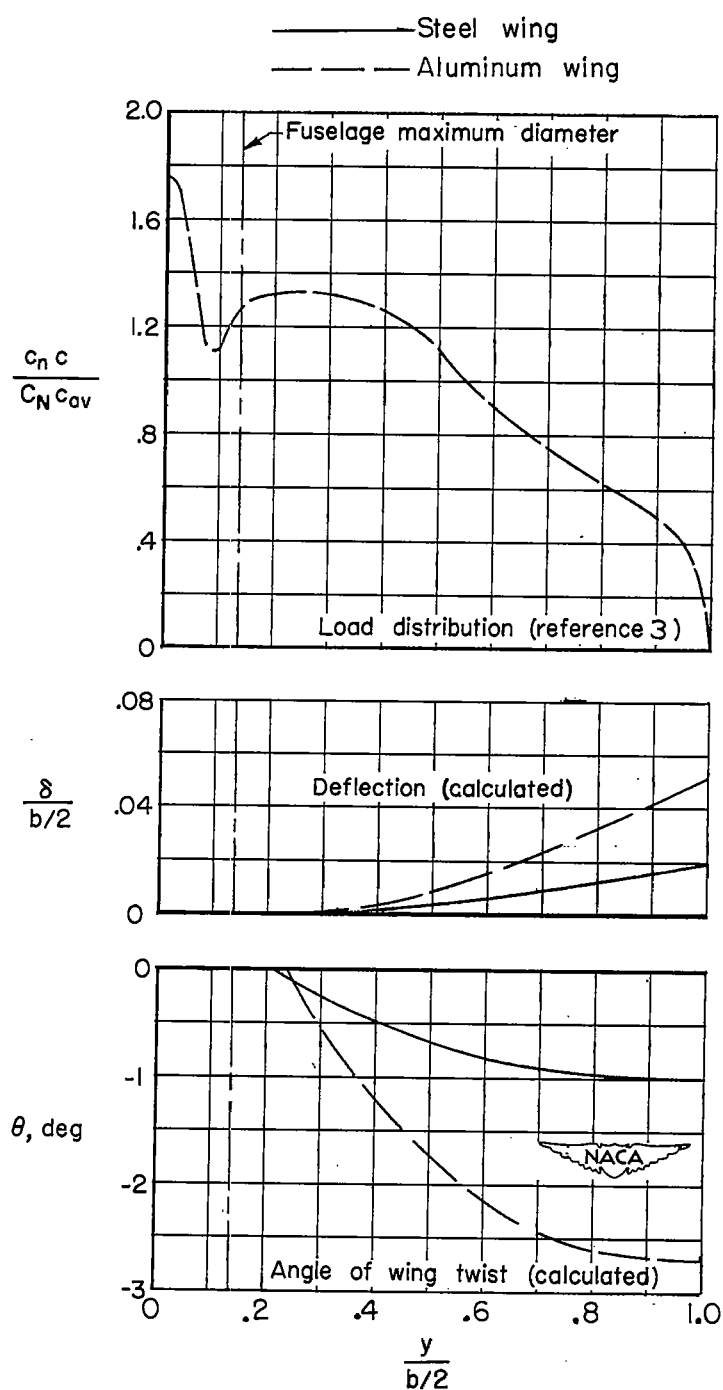
(b)  $\alpha = 20^\circ$ .

Figure 10.- Concluded.

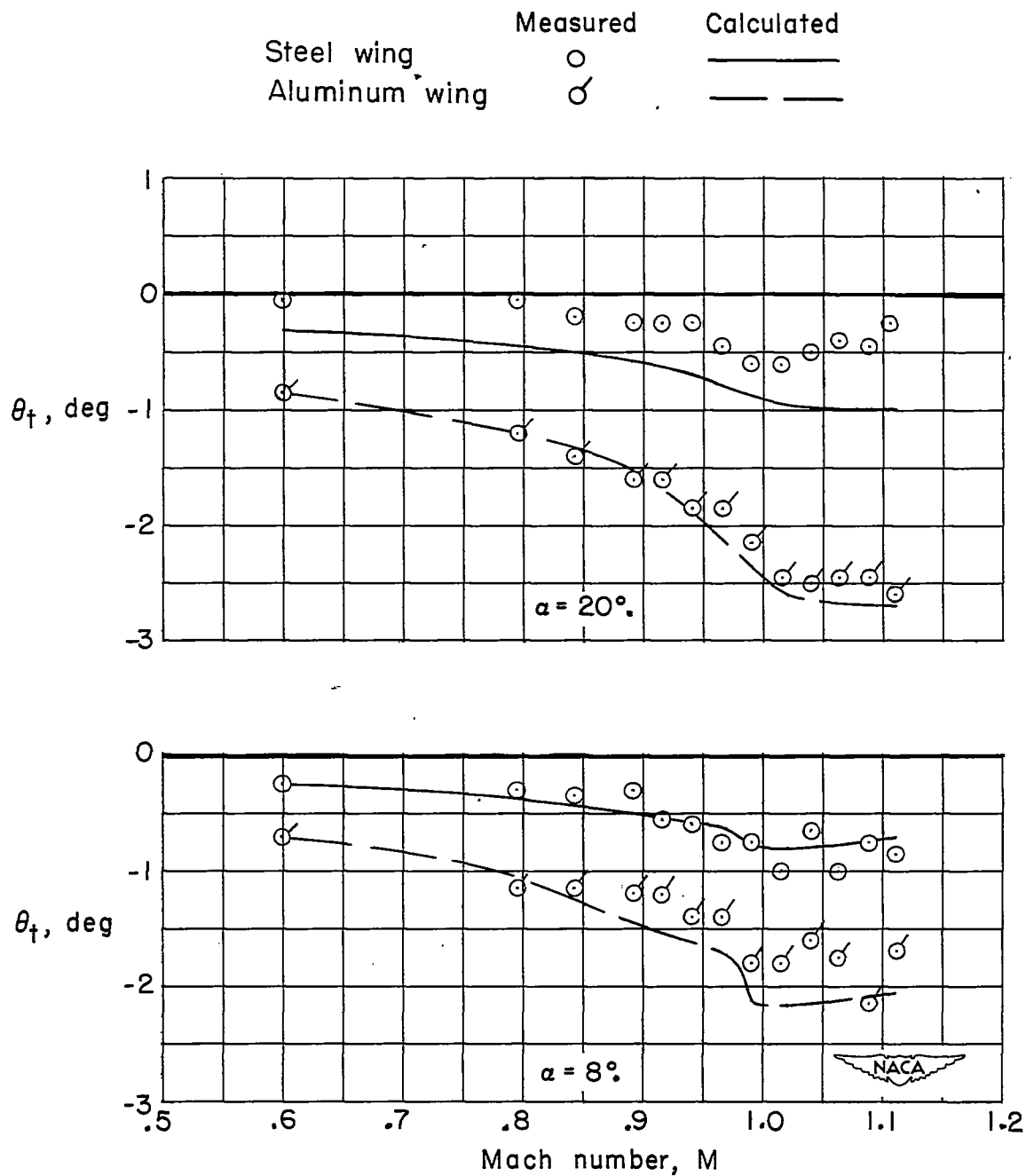


Figure 11.- Comparison of measured and calculated angles of wing-tip twist for the aluminum and steel wings.